



Functional evaluation of 16 SCHAD missense variants: Only amino acid substitutions causing congenital hyperinsulinism of infancy lead to loss-of-function phenotypes in vitro

Kelly Velasco¹  | Johanna L. St-Louis¹ | Henrikke N. Hovland¹ | Nels Thompson¹ | Åsta Ottesen¹ | Man Hung Choi^{1,2} | Line Pedersen¹ | Pål R. Njølstad^{3,4} | Thomas Arnesen^{5,6,7} | Karianne Fjeld^{1,8} | Ingvild Aukrust^{3,8} | Line M. Myklebust^{5,6} | Anders Molven^{1,2,3} 

¹Gade Laboratory for Pathology, Department of Clinical Medicine, University of Bergen, Bergen, Norway

²Department of Pathology, Haukeland University Hospital, Bergen, Norway

³Center for Diabetes Research, Department of Clinical Science, University of Bergen, Bergen, Norway

⁴Department of Pediatrics and Adolescent Medicine, Haukeland University Hospital, Bergen, Norway

⁵Department of Biomedicine, University of Bergen, Bergen, Norway

⁶Department of Biological Sciences, University of Bergen, Bergen, Norway

⁷Department of Surgery, Haukeland University Hospital, Bergen, Norway

⁸Department of Medical Genetics, Haukeland University Hospital, Bergen, Norway

Correspondence

Anders Molven, Gade Laboratory for Pathology, Department of Clinical Medicine, Haukeland University Hospital, University of Bergen, N-5021 Bergen, Norway.

Email: anders.molven@uib.no

Communicating Editor: Sander M Houten

Funding information

Helse Vest Regionalt Helseforetak, Grant/Award Number: HV 912258; Norges Forskningsråd, Grant/Award Number: FRIMEDBIO 240788; Novo Nordisk Fonden, Grant/Award Number: NNF15OC0016330

Abstract

Short-chain 3-hydroxyacyl-CoA dehydrogenase (SCHAD), encoded by the *HADH* gene, is a ubiquitously expressed mitochondrial enzyme involved in fatty acid oxidation. This protein also plays a role in insulin secretion as recessive *HADH* mutations cause congenital hyperinsulinism of infancy (CHI) via loss of an inhibitory interaction with glutamate dehydrogenase (GDH). Here, we present a functional evaluation of 16 SCHAD missense variants identified either in CHI patients or by high-throughput sequencing projects in various populations. To avoid interactions with endogenously produced SCHAD protein, we assessed protein stability, subcellular localization, and GDH interaction in a SCHAD knockout HEK293 cell line constructed by CRISPR-Cas9 methodology. We also established methods for efficient SCHAD expression and purification in *E. coli*, and tested enzymatic activity of the variants. Our analyses showed that rare variants of unknown significance identified in populations generally had similar properties as normal SCHAD. However, the CHI-associated variants p.Gly34Arg, p.Ile184Phe, p.Pro258Leu, and p.Gly303Ser were unstable with low protein levels detectable when

This is an open access article under the terms of the Creative Commons Attribution License, which permits use, distribution and reproduction in any medium, provided the original work is properly cited.

© 2020 The Authors. *Journal of Inherited Metabolic Disease* published by John Wiley & Sons Ltd on behalf of SSIEM.

expressed in HEK293 cells. Moreover, CHI variants p.Lys136Glu, p.His170Arg, and p.Met188Val presented normal protein levels but displayed clearly impaired enzymatic activity in vitro, and their interaction with GDH appeared reduced. Our results suggest that pathogenic missense variants of SCHAD either make the protein target of a post-translational quality control system or can impair the function of SCHAD without influencing its steady-state protein level. We did not find any evidence that rare SCHAD missense variants observed only in the general population and not in CHI patients are functionally affected.

KEYWORDS

congenital hyperinsulinism of infancy, *HADH*, loss-of-function mutations, SCHAD, short-chain 3-hydroxyacyl-CoA dehydrogenase, variants of unknown significance

1 | INTRODUCTION

An increasing challenge of clinical medicine is how to handle the wealth of information provided by high-throughput genetic analyses. For a given patient, techniques such as whole-exome and whole-genome sequencing may reveal multiple, rare genetic variants that are of unknown significance with regard to health implications.¹ Predicting the functional effect based on bioinformatics analyses alone is still unreliable, particularly for missense mutations; that is, when the genetic variant results in amino acid substitutions at the protein level. This problem has, for example, been illustrated by studies of *HNFI1A* variants implicated in monogenic diabetes.²

A concerted effort to functionally evaluate missense variants of the *HADH* gene has so far not been performed. This gene encodes short-chain 3-hydroxyacyl-CoA dehydrogenase (SCHAD; EC 1.1.1.35), a mitochondrial protein expressed in all cells. It exerts a general metabolic function by catalyzing the third step of β -oxidation of short- and medium-chain fatty acids.³ In addition, SCHAD has a specific role in glucose homeostasis by inhibiting insulin secretion in the pancreatic β -cells,⁴⁻⁷ most likely through an inhibitory effect on the activity of another metabolic enzyme: glutamate dehydrogenase (GDH).^{8,9} Thus, a number of recessive mutations in the *HADH* gene have been found to cause congenital hyperinsulinism of infancy (CHI; OMIM # 609975).¹⁰⁻¹² CHI is a disease characterized by inappropriately elevated plasma concentrations of insulin, resulting in episodes of hypoglycemia that may become life-threatening if not treated correctly.^{13,14}

The gnomAD data set contains 155 *HADH* missense variants, of which 154 are rare with an allele frequency < 0.01.¹⁵ Only few of the SCHAD-CHI case reports have examined protein expression and enzymatic

activity of the mutation in question.^{10,16,17} In addition, a study of the *C. elegans* SCHAD protein experimentally evaluated the structural and functional impact of two amino acid substitutions in the conserved dimerization interface of the protein.¹⁸

Here we have initiated a systematic assessment of SCHAD amino acid substitutions by establishing a toolkit of prokaryotic and eukaryotic expression vectors for producing the protein variants as well as a SCHAD knockout cell line for functional testing. We have tested 16 naturally occurring missense variants for stability, subcellular localization, enzymatic activity and GDH interaction. Overall, our data showed that SCHAD variants reported in CHI patients display various loss-of-function phenotypes, whereas functional defects were not seen in any rare variant of the general population.

2 | MATERIALS AND METHODS

2.1 | Plasmids

The complete coding sequence of the human *HADH* gene (transcript variant 2, NCBI reference sequence NM_005327.4) was synthesized (DNA 2.0) flanked by sites for the restriction enzymes *EcoRI* and *XhoI*. For eukaryotic SCHAD expression, the synthetic gene was transferred to expression vector pcDNA3.1/V5-His B (Invitrogen). The insert was cloned in-frame with the C-terminal V5/His tag using *EcoRI/XhoI* and the Quick Ligation Kit (NEB).

For prokaryotic expression, the synthetic gene served as template to amplify *HADH* without the mitochondrial import signal. Overhangs with *BsmI* and *NcoI* sites were added in the 5'-end and an *Acc65I* site in the 3'-end. PCR

primers were 5'-CATCATCGTCTCCCATGGGATCC-TCCCTCGTCCAC-3' and 5'-CATCATGGTACCATCA-CTTGATTTGTAAAATCCTTCTC-3'. Phusion High-Fidelity PCR polymerase (Thermo Fisher Scientific) was used with annealing at 53.2°C for 20 seconds. The PCR product was blunt-end-cloned into the vector pJet1.2 (CloneJET PCR Cloning Kit, Thermo Fisher Scientific). Subsequently, the *HADH* insert of the pJet1.2 vector was ligated to the pETM41-His/MBP expression vector in-frame with an N-terminal 6His/Maltose Binding Protein (MBP) tag (Quick Ligation Kit). Restriction enzymes *Acc65I/BsmBI* were used for the insert and *Acc65I/NcoI* for the vector.

Sixteen missense variants chosen from the gnomAD data set¹⁵ (transcript ENST00000309522) and from CHI case reports were introduced in the plasmids by using the QuickChange II XL Site Directed Mutagenesis Kit (Agilent). This kit was also used to delete the SCHAD mitochondrial import signal (Δ 2-12 construct). Primers used to produce each variant are listed in Table S1.

The plasmid Plu-CMV-hGDH for over-expressing human GDH was kindly provided by Dr Charles Stanley, Philadelphia.

For propagation, all plasmids were heat shock-transformed into One Shot TOP10 competent *E. coli*. Plasmids were prepared by the QIAfilter Plasmid Midi Kit (QIAGEN) and controlled by linearization/agarose gel electrophoresis and Sanger sequencing.

Empty vector (EV) pcDNA3.1/V5-His B was used as negative control in the expression studies. Theoretical molecular masses were estimated using the ProtParam tool on the ExPASy server.¹⁹ All sequence analyses for site-directed mutagenesis and for CRISPR-Cas9 genome editing (below) were performed by the SnapGene software (GSL Biotech).

2.2 | Antibodies

To detect SCHAD protein by western blotting, different polyclonal antibodies were used: rabbit anti-SCHAD (Atlas Antibodies, HPA039588; GeneTex, GTX105167) and goat anti-SCHAD (Novus Biologicals, NB100-77343). A custom-made monoclonal mouse anti-SCHAD antibody (epitope QTEDILAKSK) from Abmart was employed in some experiments. Mouse anti-V5 (R960-25), anti-mouse HRP conjugate (626520), anti-rabbit HRP conjugate (656120), anti-mouse Alexa Fluor 488 conjugate (A-11017), and goat anti-GLUD1/2 (PA5-19267) were from Thermo Fisher Scientific. Rabbit anti- β -tubulin (ab6046) and anti- β -catenin (ab32572) were from Abcam. Mouse IgG2a (X0943) was from DAKO.

2.3 | Establishment of a HEK293 SCHAD knockout (KO) cell line by CRISPR-Cas9

The gRNAs 5'-CACCGCACGGAACGCATGAACTGCC-3' and 5'-AAACGGCAGTTCATGCGTCCCGTGC-3', targeting the sequence 5'-CCAGGCAGTTCATGCGTCCCGTG-3' in the proximity of the *HADH* start codon were designed via the website <http://crispr.mit.edu>. After phosphorylation by T4 polynucleotide kinase, the gRNAs were kept at 95°C for 5 minutes, annealed by decreasing the temperature to 25°C (rate: 5°C/min), ligated into the pSpCas9(BB)-2A-Puro (PX459 v.2) plasmid (Addgene) using *BbsI* sites, and transformed into One Shot TOP10 competent *E. coli*. Plasmid preparations were sequenced using the primer 5'-GAGGGCCTATTTCCCATGATT-3'. Human embryonic kidney (HEK293) cells (Clontech) were transfected for 48 hours using the calcium phosphate method. Cells carrying plasmid were then selected using 3 μ g/mL puromycin in the growth medium for 96 hours. Surviving cells were detached with trypsin, and single cells were hand-picked and transferred to individual wells in a 96-well plate. *HADH* exon 1 was sequenced in surviving clones using the primers 5'-TCAACGCTGGGACGTTACA-3' and 5'-GTGAAAACCCCTGGTGTGCG-3'. Finally, SCHAD expression in the generated cell lines was evaluated by western blotting.

2.4 | HEK293 cell culture, SCHAD-V5 plasmid expression, western blotting

HEK293 cells (WT and SCHAD KO) were cultured in DMEM medium supplemented with 10% FBS (Gibco) and PenStrep (Sigma-Aldrich), and maintained in 5% CO₂ at 37°C. Unless indicated otherwise, Lipofectamine 2000 (Thermo Fisher Scientific) was used for transfection.

Treatment with the proteasome inhibitor MG132 (Sigma-Aldrich) was done 24 hours after transfection. The culture medium was removed, and cells were incubated with 5 μ M MG132 or an equivalent volume of DMSO in fresh medium for the specified amount of time.

To produce HEK293 whole-cell lysates, cells were incubated in RIPA buffer (Thermo Fisher Scientific) and centrifuged at 14 000g for 15 minutes at 4°C to obtain a clear supernatant. Protein concentration was measured using the Pierce BCA protein assay kit (Thermo Fisher Scientific).

For western blotting, the samples were mixed with loading buffer and reducing agent, heated at 70°C for 10 minutes and subjected to SDS-PAGE before transfer to a PVDF membrane. The proteins of interest were detected using specific antibodies and visualized by

enhanced chemiluminescence using Amersham ECL Prime Western Blotting detection reagent (GE Healthcare) and a GBOX I Chemi XR5 imager (Syngene).

2.5 | Cell-free expression of SCHAD-V5 plasmids

Cell-free expression of SCHAD variants was achieved by incubating the pcDNA3.1-SCHAD-V5-His plasmids in TNT T7 Quick Coupled Transcription/Translation master mix (Promega). Each reaction was incubated for 90 minutes at 30°C, and 3 μ L were analyzed by western blotting.

2.6 | Immunostaining and microscopy

HEK293 SCHAD KO cells were grown on poly-L-lysine coated glass coverslips. To label the mitochondria, cells were incubated for 30 minutes in 200 nM MitoTracker Red CMXRos (Invitrogen) diluted in pre-warmed cell medium. Cells were fixed for 15 minutes with 4% paraformaldehyde, permeabilized with 0.2% Triton X-100 in PBS and blocked with 1% BSA, 22.5 mg/mL glycine, 0.1% Tween in PBS. To stain for SCHAD-V5, the cells were incubated consecutively with the anti-V5 and anti-mouse Alexa Fluor 488 conjugate antibodies. Each incubation was 1 hour at room temperature, with three PBS washes of 5 minutes in between. Coverslips were mounted in ProLong Gold Antifade Reagent with DAPI (Cell Signaling Technology). The confocal images were collected using a TCS SP5 confocal microscope with a 63 \times /1.4NA HCX Plan-Apochromat oil immersion objective, \sim 1.0 airy unit pinhole aperture, and appropriate filter combinations (Leica Microsystems). Images were acquired with 405 diode, argon and DPSS 561 lasers and processed using the LAS AF software.

2.7 | MBP-SCHAD protein expression and purification

MBP-SCHAD plasmids were transformed into BL-21 (DE3) *E. coli* cells (NEB) by the heat shock method. A single colony was inoculated and grown in LB medium with 1% glucose and 50 μ g/mL kanamycin at 37°C. Protein expression was induced at OD₆₀₀ = 0.6 by adding 0.1 mM IPTG. Bacteria were harvested after overnight incubation at 22°C and sonicated in a pH 7.8 buffer (50 mM NaH₂PO₄, 500 mM NaCl, 10 mM imidazole,

0.1 mM DTT, 10% glycerol) complemented with EDTA-free protease inhibitors (Roche). Recombinant SCHAD protein was purified by immobilized metal affinity chromatography (IMAC) on a HisTrap HP 5-mL column (GE Healthcare) followed by size exclusion chromatography (SEC) on a Superdex 200 16/60120-mL column (GE Healthcare). Buffers (pH 7.8) were as follows: IMAC wash buffer (50 mM NaH₂PO₄, 300 mM NaCl, 20 mM imidazole, 0.1 mM DTT, 10% glycerol), IMAC elution buffer (= wash buffer with 250 mM imidazole), SEC buffer (50 mM NaH₂PO₄, 150 mM NaCl, 0.1 mM DTT, 10% glycerol). Fractions were analyzed by SDS-PAGE and Coomassie staining (SimplyBlue SafeStain, Invitrogen) and protein concentration was determined by A₂₈₀ measurements.

2.8 | Multiangle light scattering measurements

The molecular mass of MBP-SCHAD was calculated by SEC-MALS using a Superdex 200 HR 10/30 column coupled to a light-scattering device. Bovine serum albumin (BSA) was used as standard.

2.9 | SCHAD enzymatic assay

The enzymatic reaction was started by adding 0.07 μ g of purified MBP-SCHAD protein to 1.0 mL 100 mM potassium phosphate buffer (pH 7.0) containing 0.1 mM DTT, 0.3 mg/mL BSA (fatty acid-free) and saturating concentrations of acetoacetyl-CoA (50 μ M) and NADH (0.15 mM). Absorbance at 340 nm was measured every minute for 5 minutes at 37°C.

2.10 | Co-immunoprecipitation (co-IP)

HEK 293 SCHAD KO cells seeded in 10-cm Petri dishes were co-transfected with 2 μ g Plu-CMV-hGDH and 6 μ g of pcDNA3.1-SCHAD-V5-His variants using the calcium phosphate method. After 48 hours of transfection, cells were washed with PBS, incubated for 10 minutes with 1 mM disuccinimidyl glutarate and quenched for 15 minutes with 50 mM Tris, pH 7.5. Immediately after, co-IP was performed as follows (kit from Thermo Fisher Scientific): 6 μ g of antibody were coupled to 10 μ L AminoLink Plus Coupling resin, co-IP buffer was used for cell lysis (500 μ L/plate) and washing (\times 7), 450 μ L of cell lysate at 2.8 μ g/ μ L were incubated for 1 hour with the antibody-coupled-resin, and elution (\times 1) was by

NuPAGE LDS Sample buffer (Thermo Fisher Scientific), followed by western blotting.

2.11 | Statistical analysis

The software R²⁰ with reshape2²¹ and multcomp²² was used. Plots were produced using the package ggplot2.²³ To evaluate differences in the enzymatic activity of the SCHAD variants, a one-way analysis of variance (ANOVA) and a post-hoc Dunnett's test were used. To evaluate differences in the amount of bound GDH, a one-sample *T*-test was used.

3 | RESULTS

3.1 | Selection of SCHAD variants for functional testing

To perform a systematic functional evaluation of SCHAD protein variants, we chose 16 missense variants present in human populations and CHI patients (Table 1). The population variants were selected to be distributed throughout the domains of SCHAD, and their positions are illustrated in Figures 1A and S1A. Specifically, nine

variants were selected from the gnomAD data set,¹⁵ most of them having an allele frequency in the range 0.0002 to 0.005 (Table 1). We also included p.Pro86Leu, which is the most frequent SCHAD coding variant and the only one with an allele frequency > 0.01.²⁷ Additionally, seven pathogenic variants found in CHI cases were included. Of these, six have been described in case reports^{10,16,17,24-26} whereas one, p.His170Arg, has been identified in a CHI patient via our own clinical laboratory service (unpublished).

To characterize functional aspects of these variants *in vitro*, we introduced them by site-directed mutagenesis into plasmids pcDNA3.1 (for expression in mammalian cells as SCHAD-V5/His fusion protein) and pETM41-His/MBP (for expression in *E. coli* as MBP-SCHAD fusion protein).

3.2 | Expression of SCHAD missense variants in HEK293 cells

SCHAD is a ubiquitous protein that occurs as homodimer in its functional form.^{18,28} To avoid the interference that dimerization with endogenous wildtype protein could cause in cellular studies with exogenously expressed variants, we produced a HEK293 SCHAD KO cell line using

TABLE 1 Overview of *HADH* variants and the studied amino acid substitutions

Nucleotide change ^a	Amino acid variant ^b	Exon	Reference SNP ID number ^c	Allele frequency ^d	Source
c.99C > G	p.Ile33Met	1	rs74428123	0.00040	gnomAD
c.100G > C	p.Gly34Arg	1	rs779135938	0.00001	24
c.171C > A	p.Asp57Glu	2	rs137853102	0.00001	gnomAD
c.257C > T	p.Pro86Leu	2	rs4956145	0.08480	gnomAD
c.275 T > G	p.Phe92Cys	3	rs61735992	0.00568	gnomAD
c.406A > G	p.Lys136Glu	3	rs1262186453	0.00003	25
c.456G > T	p.Gln152His	4	rs1051519	0.00175	gnomAD
c.509A > G	p.His170Arg	4	—	—	Unpublished ^e
c.550A > T	p.Ile184Phe	5	—	—	26
c.562A > G	p.Met188Val	5	—	—	16
c.614G > C	p.Gly205Ala	5	rs144699575	0.00023	gnomAD
c.643C > A	p.Pro215Thr	6	rs140413151	0.00184	gnomAD
c.662G > A	p.Arg221His	6	rs76476980	0.00117	gnomAD
c.773C > T	p.Pro258Leu	7	rs137853103	—	10
c.881A > G	p.Asn294Ser	8	rs36030668	0.00235	gnomAD
c.907G > A	p.Gly303Ser	8	rs201772964	0.00004	17

^aAccording to NCBI reference sequence NM_005327.4.

^bPredicted amino acid change. Notation according to NCBI reference sequence NP_005318.3.

^cAccording to the Single Nucleotide Polymorphism Database (dbSNP) (<https://www.ncbi.nlm.nih.gov>).

^dAccording to the gnomAD database (<http://gnomad.broadinstitute.org>).¹⁵

^eUnpublished patient from own clinical laboratory service.

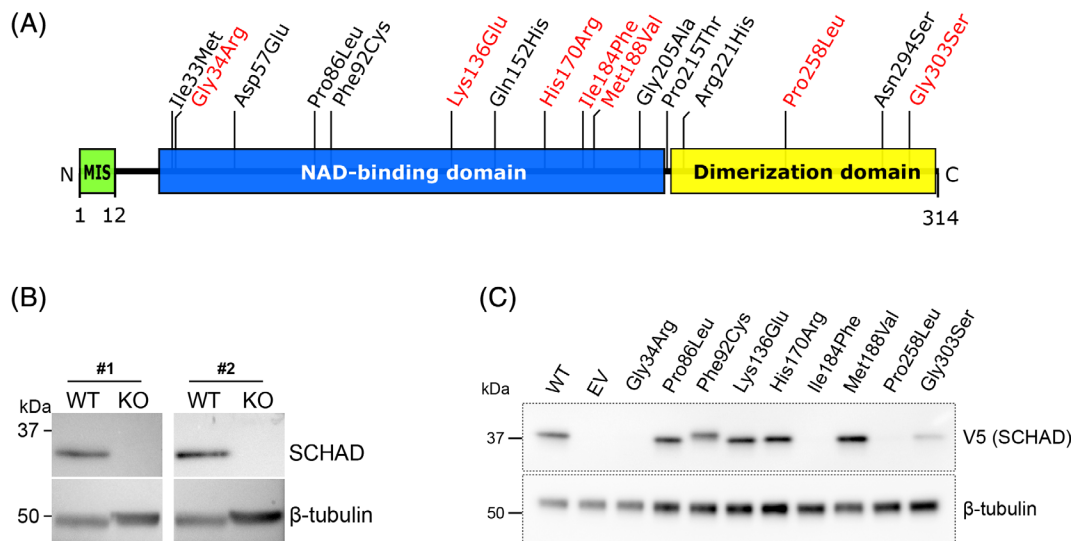


FIGURE 1 Location of the studied missense variants in the SCHAD protein, construction of SCHAD-deficient HEK293 cells, and expression of selected variants in these cells. A, SCHAD has three functional domains: the mitochondrial import signal (MIS; green), the NAD-binding domain (blue) and the dimerization domain (yellow). Protein variants of unknown significance found in populations are in black, while pathogenic variants found in CHI patients are displayed in red. Notation is according to the reference protein sequence NP_005318.3. For simplicity, the prefix “p.” of the amino acid variants is not included in this and the other figures. B, Western blot of cell lysates from HEK293 cells expressing (wildtype, WT) and not expressing (knockout, KO) SCHAD protein. Membranes were probed with two different anti-SCHAD antibodies (#1, GeneTex; #2, Novus Biologicals). C, Western blot of whole-cell lysates of HEK293 SCHAD KO cells transfected with the indicated variants. One μg of protein was loaded in each lane, and the SCHAD variants were detected with anti-V5 antibody. A representative image of three experiments is shown. An anti- β -tubulin antibody was used for monitoring the loading in B and C. EV = empty vector

CRISPR-Cas9 targeted genome editing. Disruption of exon 1 of the *HADH* gene was verified through DNA sequencing of selected colonies (Figure S2). Knockout at the protein level was confirmed through western blotting using different anti-SCHAD antibodies (Figure 1B). A band of the expected molecular mass for SCHAD (~34 kDa) was observed only for the lysates of HEK293 WT cells, and not for SCHAD KO cells.

We then tested expression of the SCHAD variants by transiently transfecting the plasmids into HEK293 SCHAD KO cells. Figure 1C shows selected variants in HEK293 SCHAD KO cells to summarize the most relevant findings, whereas Figure S3 presents all 16 variants expressed in both HEK293 WT and SCHAD KO cells. Analysis of the cellular lysates by western blotting, using an anti-V5 antibody (Figure 1C) or an anti-SCHAD antibody (Figure S3), revealed a band of the expected molecular mass (~37 kDa) for the WT-V5/His fusion protein. Most missense variants exhibited the same size and expression levels as the WT protein. The five exceptions were p.Gly34Arg, p.Phe92Cys, p.Ile184Phe, p.Pro258Leu, and p.Gly303Ser. The p.Phe92Cys variant, found in the gnomAD dataset, displayed slower electrophoretic mobility than the WT protein, but had the same expression level. The four other variants, all CHI-associated, were

consistently expressed at reduced levels. This reduction was more pronounced for p.Gly34Arg, p.Ile184Phe, and p.Pro258Leu than for the p.Gly303Ser variant. However, CHI variants p.Lys136Glu, p.His170Arg, and p.Met188Val appeared similar to the WT protein and the remaining population variants. All 16 variants yielded the same expression pattern in normal HEK293 (WT) as in the SCHAD KO cell line (Figure S3).

Next, we evaluated the expression and subcellular localization of the variants by immunofluorescence of transiently transfected KO cells. Figure 2 exemplifies how variants exhibiting reduced protein levels in Figure 1C, such as p.Pro258Leu and p.Gly303Ser, also resulted in lower amounts of SCHAD-V5 when directly visualized in the cells. Images of the other variants are presented in Figure S4. For variants with lower protein levels, we did not observe a uniform overall reduction in SCHAD levels within the expressing cells. A few cells displayed a fluorescence pattern comparable to that of WT-transfected cells, while most cells showed from very low to undetectable SCHAD levels.

By confocal microscopy, we found that all variants were correctly targeted to the mitochondria as shown by co-localization of SCHAD-V5 with a mitochondrial-specific stain (Figure S5).

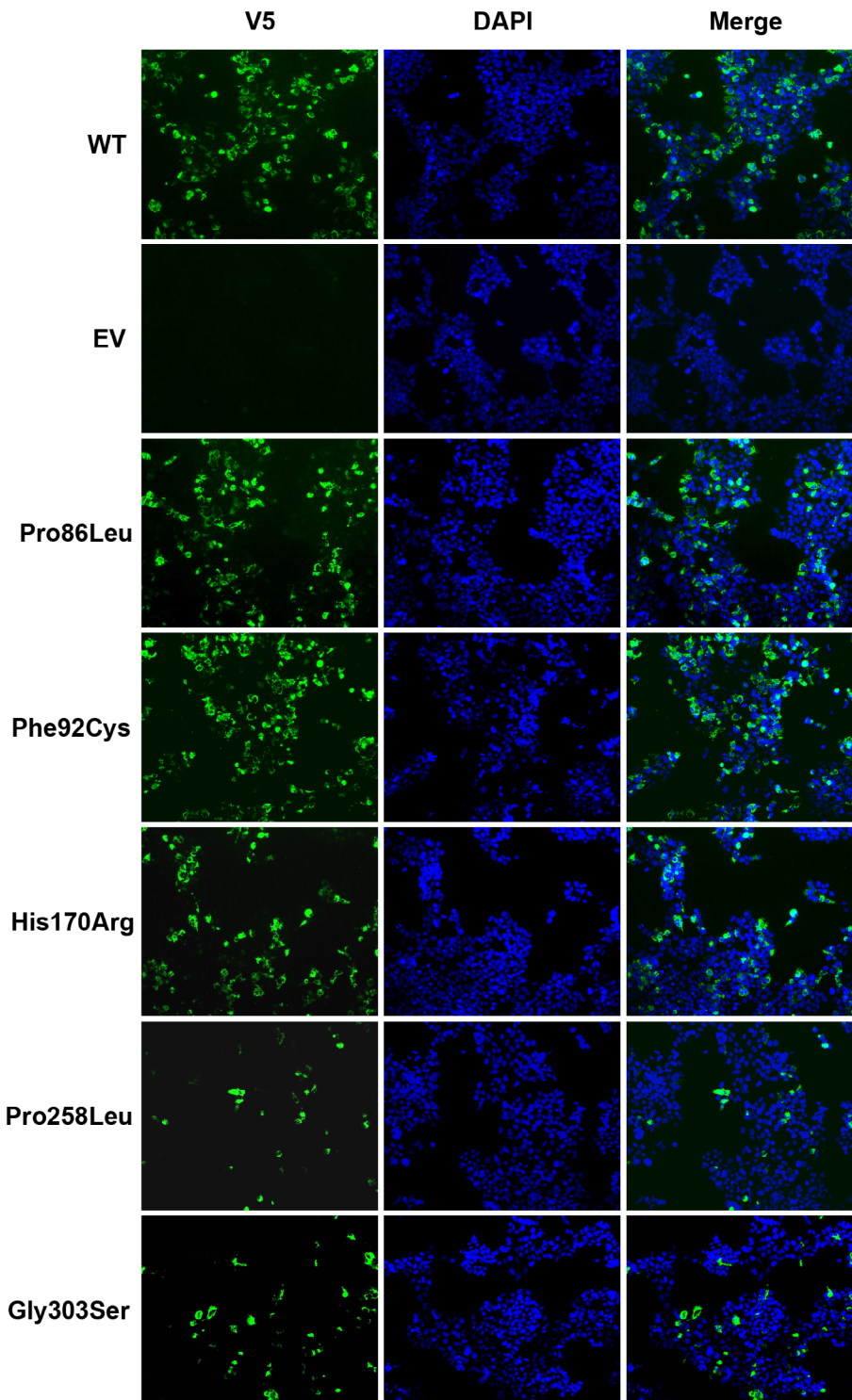


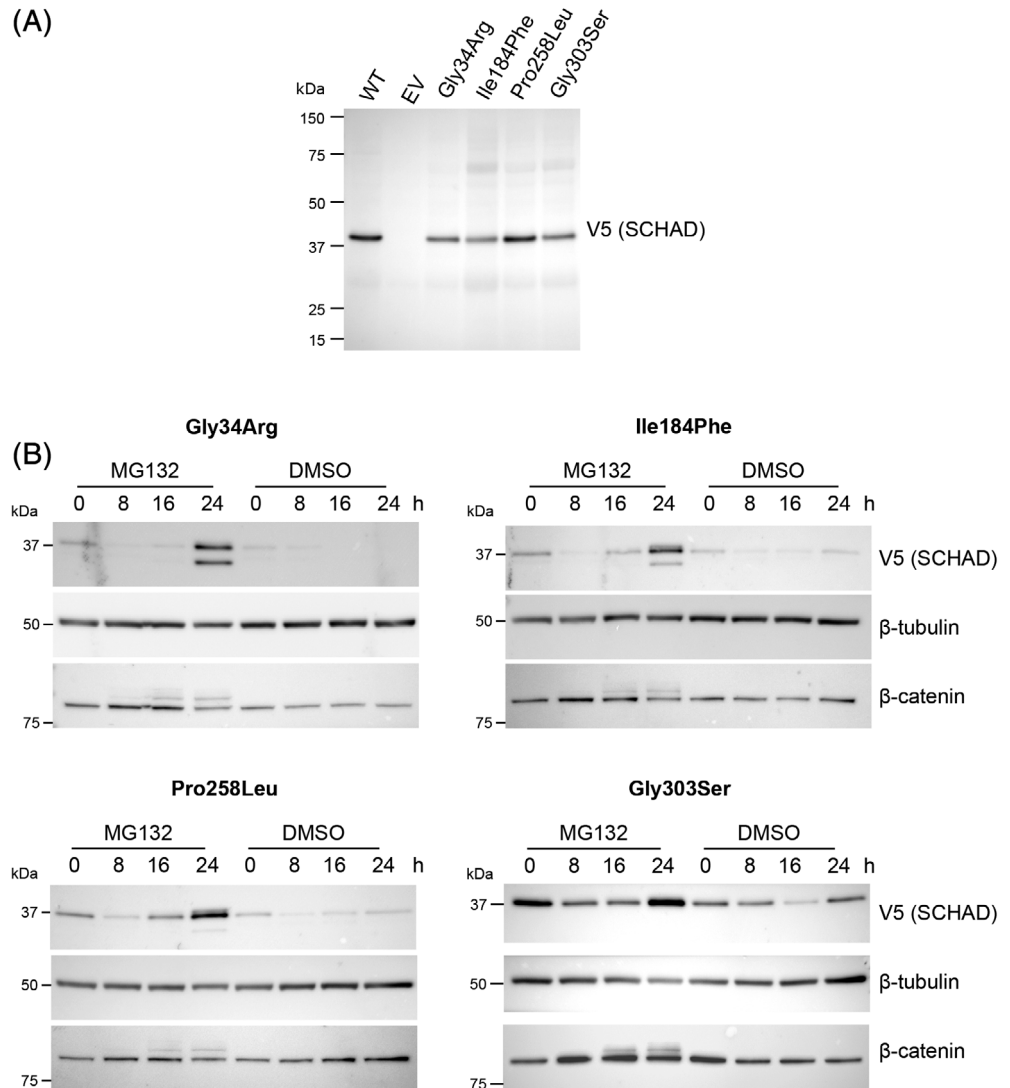
FIGURE 2 Expression of selected SCHAD variants in HEK293 SCHAD KO cells as determined by immunofluorescence. The cells were transiently transfected with the indicated V5-tagged SCHAD variants, fixed 48 hours-post transfection, stained using anti-V5 primary antibody and fluorescent anti-mouse IgG secondary antibody (green), and counterstained with DAPI (blue). Images are representative fields from two experiments, each with two technical replicates ($\times 200$). WT = wildtype, EV = empty vector

3.3 | Translation and protein degradation of SCHAD variants with reduced protein levels

To further test expression of variants p.Gly34Arg, p.Ile184Phe, p.Pro258Leu, and p.Gly303Ser, that is, those displaying low protein levels in HEK293 cells, we used a cell-free expression system. Equal amounts of the

plasmids were incubated with the cell-free expression reaction mix followed by western blotting. In stark contrast to the results obtained with transfected cells, these four variants now displayed similar protein levels to WT SCHAD (Figure 3A). This confirmed that the plasmids were fully functional with protein synthesis being as efficient as from the WT plasmid. Moreover, this observation hinted at the activity of a cellular quality control

FIGURE 3 Expression of unstable SCHAD variants in a cell-free system and in HEK293 cells treated with a proteasome inhibitor. A, Equal amounts of the vectors expressing the indicated variants were incubated with the cell-free expression master mix for 90 minutes. Three microliters of each reaction were analyzed by western blot using an anti-V5 antibody. WT = wildtype, EV = empty vector. B, Twenty-four hours after transfection with the indicated variants, HEK293 SCHAD KO cells were treated with 5 μ M MG132 or only DMSO for the specified times. To be able to visualize the unstable variants, we loaded five times the amount of whole-cell lysate (5 μ g) per well than loaded in Figure 1C. The blots were analyzed by anti-V5 antibody, whereas anti- β -tubulin and anti- β -catenin antibodies were used for monitoring the loading and controlling the efficiency of MG132 treatment, respectively



mechanism, not present in the cell-free expression system, as explanation for the low variant levels in HEK293 cells.

To investigate whether the four variants were degraded by the ubiquitin-proteasome system, we blocked this pathway in transfected cells by using the proteasome inhibitor MG132. Figure 3B demonstrates that the variants p.Gly34Arg, p.Ile184Phe, and p.Pro258Leu exhibited clearly increased protein levels after 24 hours of MG132 treatment, suggesting that proteasomal degradation is of importance for their instability. There was also a certain effect on the level of p.Gly303Ser, an increase that was confirmed in two additional, independent experiments.

3.4 | Enzymatic activity of purified SCHAD variants

Although enzymatic activity of SCHAD can be measured in cell and tissue lysates,³ we opted for using purified

protein due to the greater flexibility of the assay and full control over the amount of SCHAD tested. Even though we were able to express all variants in *E. coli* cells, the purification efficiency differed considerably from variant to variant (Figure S6 and data not shown). In fact, the levels of p.Gly34Arg, p.Phe92Cys, and p.Ile184Phe were undetectable at the end of the SEC purification step and therefore no further work was performed on them. Notably, for all variants we employed a purification protocol optimized for WT SCHAD. Thus, none of the conditions were adjusted to the individual characteristics of any specific variant as an attempt to improve the yield.

We assessed the identity and purity of the samples by SDS-PAGE, western blotting and Coomassie staining. For all purified variants, a band around 75 kDa was detected by anti-SCHAD (Figure 4A) and anti-His (data not shown) antibodies. This agrees with the predicted molecular mass of ~77 kDa for MBP-SCHAD. Coomassie staining revealed a few additional, weak bands of higher molecular mass and unknown identity in all cases

(Figure S7A). Some variants, most notably p.Ile33Met, exhibited additional bands of lower molecular weight.

To test if recombinant MBP-SCHAD was purified in the functional dimeric form, we estimated the molecular mass of purified MBP-SCHAD WT by SEC-MALS (Figure S7B). While the predicted monomeric molecular mass was ~77 kDa, the calculated value by SEC-MALS analysis was ~168 kDa. This indicated that MBP-SCHAD WT was purified in the dimeric form. As the missense variants all eluted at the same rate as WT SCHAD (Figure S6), we expected them to be purified as dimers, too.

Next, we assessed the enzymatic activity of the variants in saturating conditions of substrate and co-factor (V_{max}). MBP-SCHAD WT exhibited $V_{max} = 181 \pm 3 \mu\text{mol}/\text{min}/\text{mg}$ (Figure 4B). Variants found in patients all showed reduced activity: p.His170Arg, p.Pro258Leu,

and p.Gly303Ser had severely reduced V_{max} ($<10 \mu\text{mol}/\text{min}/\text{mg}$), while p.Lys136Glu ($127 \pm 8 \mu\text{mol}/\text{min}/\text{mg}$) and p.Met188Val ($132 \pm 29 \mu\text{mol}/\text{min}/\text{mg}$) displayed a smaller, but still significant, reduction. Interestingly, the population variant p.Pro215Thr had a slight increase in enzymatic activity ($211 \pm 5 \mu\text{mol}/\text{min}/\text{mg}$).

3.5 | Interaction of pathogenic SCHAD variants with GDH

We were therefore left with principally two classes of SCHAD pathogenic variants, one with severely reduced cellular amounts of protein and another with impaired enzymatic activity in the presence of normal protein levels. The variants of the latter class might still have the capacity to inhibit GDH, thereby carrying out normal

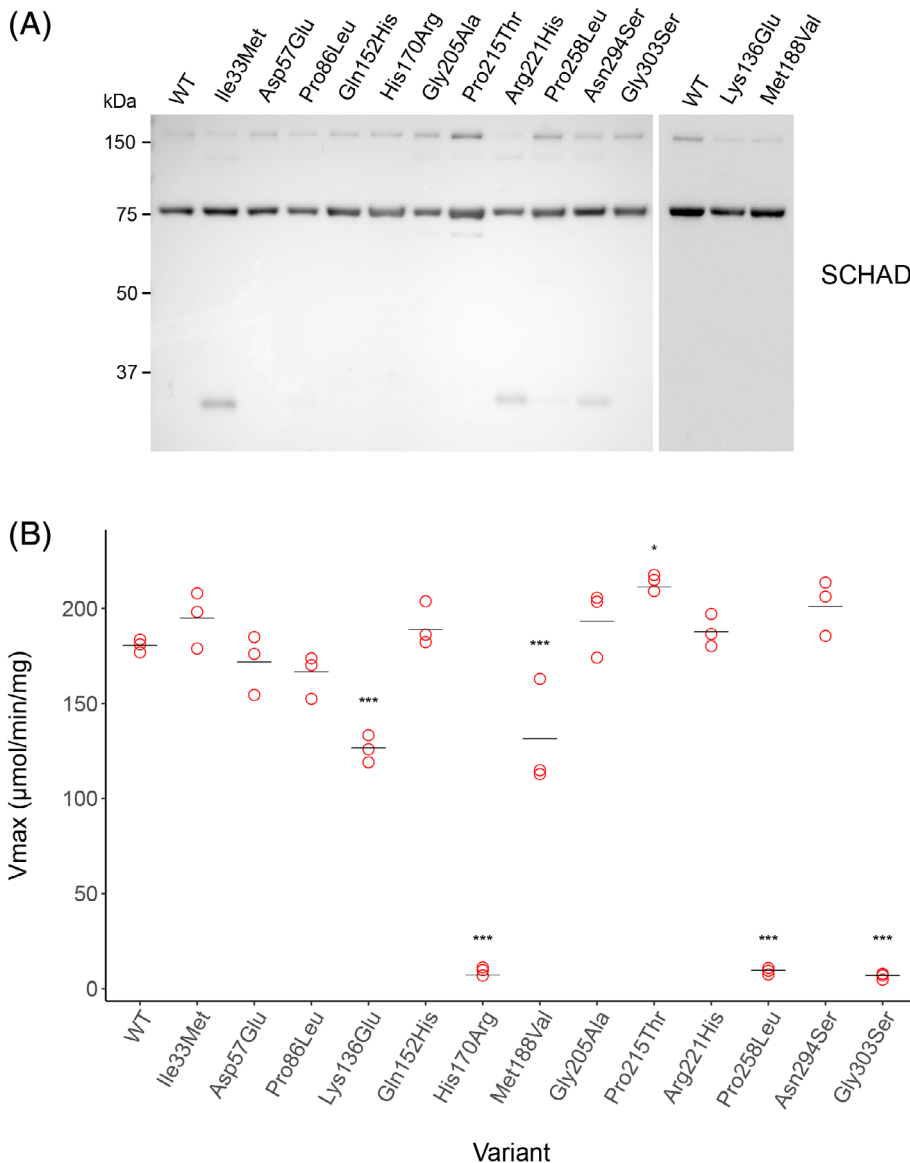


FIGURE 4 Purified recombinant MBP-SCHAD variants from *E. coli* and their enzymatic activity. A, Western blot of all successfully purified variants. Purified protein samples (0.3 μg) were analyzed using the Abmart anti-SCHAD antibody. B, The enzymatic activity of the purified variants was tested on three different days, each time with three measurements. Each dot represents the mean of a triplicate measurement and the horizontal lines show the overall mean. * $P < .05$, *** $P < .001$

SCHAD function in insulin secretion. We therefore evaluated the ability of the variants of the second class (p.Lys136Glu, p.His170Arg, and p.Met188Val) to bind GDH by using co-IP (Figures 5 and S8). We co-transfected HEK293 SCHAD KO cells with GDH and the SCHAD variant to be tested, and then treated the cells with a crosslinking reagent before cell lysis and co-IP. This ensured that we captured protein interactions within the mitochondria. The set-up was validated by including a SCHAD variant (Δ 2-12) lacking the mitochondrial import signal and therefore unable to locate with GDH inside the mitochondria. The positive control (WT SCHAD) and all negative controls (EV, Δ 2-12, IgG) behaved as intended. Somewhat unexpectedly, GDH was still able to co-IP with the three pathogenic SCHAD variants (Figure 5A, B). Nevertheless, the GDH levels were lower for the missense variants than for WT SCHAD in eight of nine independent Co-IPs tests performed (Figure 5C), although for each variant the reduction did not quite reach statistical significance when assessed separately.

4 | DISCUSSION

We here, for the first time, present a concerted functional assessment of naturally occurring SCHAD missense variants. We have evaluated protein expression, intracellular localization, enzymatic activity and GDH interaction. A strength of our study is that we used a cell line devoid of the SCHAD protein. Because this protein naturally forms dimers,^{18,28} our approach allowed the functional testing of SCHAD variants without the interference of endogenous protein.

All tested SCHAD missense variants from verified CHI patients displayed loss-of-function phenotypes. This is in line with the other CHI mutations in the literature being nonsense mutations, exon deletions or mutations that affect the splicing machinery.¹¹ Thus, pathogenic *HADH* mutations are generally predicted to result in deficiency of SCHAD protein. They are recessively inherited in all reported pedigrees (eg, References 12 and 25). One functional *HADH* allele therefore provides a level of SCHAD protein function sufficient to avoid hypoglycemic episodes, and dominant-negative mutations are yet to be described.

We found altered properties for all seven CHI-associated SCHAD variants examined. A few case reports of missense mutations have investigated SCHAD protein levels and/or enzyme activity in patient fibroblasts. Consistent with our findings, Clayton et al¹⁰ and Vilarinho et al¹⁷ observed low protein levels for the variants p.Pro258Leu and p.Gly303Ser, respectively, whereas Kapoor et al¹⁶ found decreased enzymatic activity for

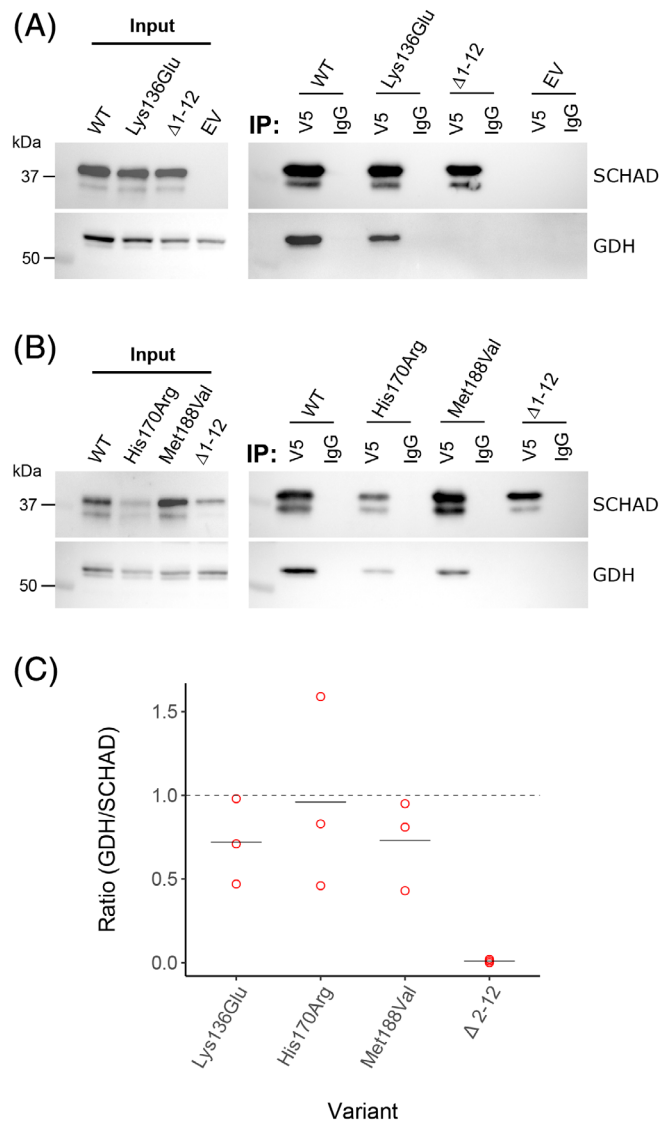


FIGURE 5 Co-immunoprecipitation of GDH with selected SCHAD variants. A,B, HEK 293 SCHAD KO cells were co-transfected with plasmids expressing GDH and selected SCHAD-V5 variants or with GDH and an empty plasmid vector (EV). The SCHAD variant Δ 2-12 lacked the mitochondrial import signal. Forty-eight hours post transfection, cells were treated with a crosslinking reagent before lysis. Cell lysates (450 μ L) with equal protein concentration (Input) were incubated with either V5 or IgG antibodies coupled to agarose beads. The proteins bound to the antibodies/beads (IP) were separated by SDS-PAGE, and SCHAD (GeneTex antibody) and GDH were visualized by western blotting. C, GDH and SCHAD western blot signals were quantified for the variants and normalized to the WT sample. The dots represent the calculated GDH/SCHAD ratio for each replicate with the horizontal lines showing the mean for each variant. The dashed line corresponds to the GDH/SCHAD ratio for the wildtype co-IP reaction

p.Met188Val. However, while we noted a drastically reduced V_{max} for recombinantly expressed and purified p.Gly303Ser, Vilarinho et al¹⁷ in patient fibroblasts

observed a V_{\max} comparable to the value of healthy controls. Still, they noted that the enzymatic function was affected by an increased K_m for binding to the co-factor NADH.

Our results suggest that SCHAD missense variants causing CHI exhibit at least two types of loss-of-function phenotypes. The first group, consisting of p.Gly34Arg, p.Ile184Phe, p.Pro258Leu, and p.Gly303Ser, displays the most common outcome for pathogenic missense mutations; that is, a decrease of the protein's half-life leading to lower amounts in the cell.²⁹ This can be explained by abnormal folding of the protein such that folding intermediates and/or improperly folded proteins are degraded through a protein-quality control system. Accordingly, we readily achieved protein expression in a cell-free eukaryotic system, and treatment with a proteasome inhibitor stabilized the protein levels in HEK293 cells. The small amounts of these variants still detectable by western blot and immunofluorescence may represent a fraction of the synthesized protein that managed to obtain a folded state and escape degradation before import to the mitochondria.³⁰

A second loss-of-function phenotype was seen for CHI variants p.Lys136Glu, p.His170Arg, and p.Met188Val. Here, enzymatic activity of SCHAD was clearly impacted, but without visible affection of steady-state protein levels. It should be pointed out, though, that biophysical stress (such as high temperature) might have demonstrated protein instability also in this group of missense variants.

Among all CHI variants studied, p.His170Arg was the most atypical since it is the only one located directly in the active site of the enzyme. The His170 residue is part of the catalytic His-Glu pair and functions as a catalytic base, involved in proton abstraction from the substrate.²⁸ In the three-dimensional conformation of SCHAD, p.Lys136 and p.Met188 are both located on the surface of the NAD-binding domain, opposite to the catalytic site (Figure S1B). Due to the nature of these amino acids and their location, they could be involved in some interaction or binding, critical for proper functioning of the protein. Notably, Xu et al¹⁸ have demonstrated that mutations distant from the catalytic site affect the enzymatic activity of *C. elegans* SCHAD by decreasing the stability of the catalytic intermediate formation. Considering that in the context of insulin regulation, SCHAD acts by inhibiting GDH,⁸ we tested this particular protein-protein interaction, expecting that pathogenic variants with normal steady-state protein levels would exhibit abolished GDH binding. However, compared with WT SCHAD we found only a partial reduction of the GDH interaction. It is therefore not obvious how these three variants result in CHI.

Of the evaluated population variants, most had properties like that of normal SCHAD. Intriguingly, the p.Asp57Glu variant has been identified in a patient with fulminant hepatic failure consistent with a metabolic disorder involving defective fatty acid oxidation. The patient was heterozygous for p.Asp57Glu, which occurred together with the variant p.Ala40Thr.³¹ In fact, a second variant in the Asp57 residue has been identified in a patient with Reye-like syndrome (p.Asp57Gly) who was compound heterozygous, carrying another unique variant, p.Tyr214His.³² Possibly, these variants could affect the function of the SCHAD protein in fatty acid oxidation but not in insulin secretion.

Among the population variants, p.Phe92Cys stood out by consistently migrating with slower electrophoretic mobility. Still, its protein level was as for WT SCHAD, and we speculate that an extra post-translational modification involving the Cys92 residue might cause the apparent increase in molecular mass. As p.Phe92Cys was the only population variant that could not be purified after *E. coli* expression, we cannot rule out an effect on enzymatic function. Still, with an allele frequency of ~0.006, this variant is the second most frequent SCHAD amino acid substitution observed in populations, and we consider it unlikely to have a pathogenic phenotype.

There is only one common variant (allele frequency > 0.01) of the *HADH* gene that results in change of protein sequence, namely p.Pro86Leu. When expression levels and enzyme activity of p.Pro86Leu were evaluated in fibroblasts of heterozygous carriers, properties comparable for non-carriers were found.²⁷ Considering that around 0.7% of the population are predicted to be homozygous for this SNP (based on allele frequency of ~0.085 according to the gnomAD database), it was interesting to test the functional effects of this variant without any interference of the WT protein. We observed no obvious difference regarding expression or enzymatic activity when compared with normal SCHAD.

The phenotype of SCHAD deficiency is different from that of other genetic disorders in which genes encoding the enzymes of fatty acid oxidation are mutated. The protein has its highest expression level in the pancreatic β -cells,⁵ and it is when the islet-specific function is disrupted that hypoglycemia ensues.⁶ Notably, a recent analysis of the genetic architecture of diabetes indicated a small, protective effect of rare variants of the *HADH* gene (Figure 2c in Reference 33), an effect that might be explained by heterozygous carriers of rare *HADH* variants having increased capacity for insulin secretion. A limitation of the present study is therefore that the amino acid substitutions were not tested in cell lines that reflect the β -cell environment, such as INS-1 or EndoC- β H1. Hence, it is conceivable that a variant that in the present

study appears normal with regard to SCHAD expression and function, still could exhibit altered properties in β -cells.

Another limitation is that we included only one of the four SCHAD variants found in patients who had no signs of hyperinsulinism but presented with other metabolic diseases (fulminant hepatic failure and Reye-like syndrome). Only the enzyme kinetics of these non-CHI variants have so far been investigated.^{31,32} It would have been interesting to investigate their properties both individually and in the combination that they appear in the patients, comparing with the CHI-causing variants. Finally, future studies should address whether the CHI variants with normal protein levels are unable to inhibit GDH despite being able to bind it, or whether these variants disturb other crucial interactions within the protein super complex in which SCHAD is postulated to be embedded.³⁴ Investigations of how GDH kinetics and protein complex formation are impacted by the normally expressed variants may be needed to fully clarify the mechanism of GDH activation in SCHAD-CHI.

Nevertheless, we have established a set of useful tools for functional testing of SCHAD protein variants. This toolkit includes a human cell line devoid of endogenous SCHAD expression as well as a series of eukaryotic/prokaryotic expression plasmids with missense variants distributed over the two major protein domains. We found no evidence that rare SCHAD amino acid substitutions not seen in CHI patients exhibited impaired function. This information will be of value when interpreting *HADH* genetic variants revealed by high-throughput sequencing projects and in clinical testing.

ACKNOWLEDGMENTS

We are indebted to Drs Charles Stanley and Changhong Li at the Children's Hospital of Philadelphia, Pennsylvania, USA for providing the plasmid Plu-CMV-hGDH and for valuable discussions. We thank Dr Sven Le Moine Bauer for assistance with statistical analyses and Dr Bjørn Dalhus, Structural Biology Core Facility, University of Oslo for assistance with the SEC-MALS analysis. The authors confirm independence from the sponsors; the content of the article has not been influenced by the sponsors.

CONFLICT OF INTEREST

The authors declare no potential conflict of interests.

ORCID

Kelly Velasco  <https://orcid.org/0000-0002-9376-6034>

Anders Molven  <https://orcid.org/0000-0003-1847-3079>

REFERENCES

- Hitomi Y, Tokunaga K. Significance of functional disease-causal/susceptible variants identified by whole-genome analyses for the understanding of human diseases. *Proc Japan Acad Ser B*. 2017;93:657-676.
- Najmi LA, Aukrust I, Flannick J, et al. Functional investigations of HNF1A identify rare variants as risk factors for type 2 diabetes in the general population. *Diabetes*. 2017;66:335-346.
- Wanders RJA, Ruiten JPN, IJlst L, Waterham HR, Houten SM. The enzymology of mitochondrial fatty acid beta-oxidation and its application to follow-up analysis of positive neonatal screening results. *J Inherit Metab Dis*. 2010;33:479-494.
- Hardy OT, Hohmeier HE, Becker TC, et al. Functional genomics of the β -cell: short-chain 3-Hydroxyacyl-coenzyme a dehydrogenase regulates insulin secretion independent of K⁺ currents. *Mol Endocrinol*. 2007;21:765-773.
- Martens GA, Vervoort A, Van De Castele M, et al. Specificity in beta cell expression of L-3-hydroxyacyl-CoA dehydrogenase, short chain, and potential role in down-regulating insulin release. *J Biol Chem*. 2007;282:21134-21144.
- Molven A, Hollister-Lock J, Hu J, et al. The hypoglycemic phenotype is islet cell-autonomous in short-chain hydroxyacyl-CoA dehydrogenase-deficient mice. *Diabetes*. 2016;65:1672-1678.
- Pepin É, Guay C, Delghingaro-Augusto V, et al. Short-chain 3-hydroxyacyl-CoA dehydrogenase is a negative regulator of insulin secretion in response to fuel and non-fuel stimuli in INS832/13 β -cells. *J Diabetes*. 2010;2:157-167.
- Li C, Chen P, Palladino A, et al. Mechanism of hyperinsulinism in short-chain 3-hydroxyacyl-CoA dehydrogenase deficiency involves activation of glutamate dehydrogenase. *J Biol Chem*. 2010;285:31806-31818.
- Smith HQ, Li C, Stanley CA, Smith TJ. Glutamate dehydrogenase, a complex enzyme at a crucial metabolic branch point. *Neurochem Res*. 2019;44:117-132.
- Clayton PT, Eaton S, Aynsley-Green A, et al. Hyperinsulinism in short-chain L-3-hydroxyacyl-CoA dehydrogenase deficiency reveals the importance of β -oxidation in insulin secretion. *J Clin Invest*. 2001;108:457-465.
- Molven A, Helgeland G, Sandal T, Njølstad PR (2012) The molecular genetics and pathophysiology of congenital hyperinsulinism caused by short-chain 3-hydroxyacyl-coA dehydrogenase deficiency. In: Stanley CA, De Leon DD (eds) *Monogenic Hyperinsulinemic Hypoglycemia Disorders*. *Frontiers in Diabetes*. Karger, Basel, pp. 137-145.
- Molven A, Matre GE, Duran M, et al. Familial hyperinsulinemic hypoglycemia caused by a defect in the SCHAD enzyme of mitochondrial fatty acid oxidation. *Diabetes*. 2004; 53:221-227.
- Arnoux JB, Verkarre V, Saint-Martin C, et al. Congenital hyperinsulinism: current trends in diagnosis and therapy. *Orphanet J Rare Dis*. 2011;6:1-14.
- Stanley CA. Perspective on the genetics and diagnosis of congenital hyperinsulinism disorders. *J Clin Endocrinol Metab*. 2016;101:815-826.
- Karczewski KJ, Francioli LC, Tiao G, et al. The mutational constraint spectrum quantified from variation in 141,456 humans. *Nature*. 2020;581:434-443.
- Kapoor RR, James C, Flanagan SE, Ellard S, Eaton S, Hussain K. 3-Hydroxyacyl-coenzyme a dehydrogenase deficiency and hyperinsulinemic hypoglycemia: characterization of a novel mutation and severe dietary protein sensitivity. *J Clin Endocrinol Metab*. 2009;94:2221-2225.

17. Vilarinho L, Sales Marques J, Rocha H, et al. Diagnosis of a patient with a kinetic variant of medium and short-chain 3-hydroxyacyl-CoA dehydrogenase deficiency by newborn screening. *Mol Genet Metab.* 2012;106:277-280.
18. Xu Y, Li H, Jin Y-H, Fan J, Sun F. Dimerization interface of 3-hydroxyacyl-CoA dehydrogenase tunes the formation of its catalytic intermediate. *PLoS One.* 2014;9:e95965.
19. Artimo P, Jonnalagedda M, Arnold K, et al. ExPASy: SIB bioinformatics resource portal. *Nucleic Acids Res.* 2012;40:597-603.
20. R Core Team. *R: A Language and Environment for Statistical Computing.* Vienna: R Foundation for Statistical Computing; 2017.
21. Wickham H. Reshaping data with the {reshape} package. *J Stat Softw.* 2007;21:1-20.
22. Hothorn T, Bretz F, Westfall P. Simultaneous inference in general parametric models. *Biom J.* 2008;50:346-363.
23. Wickham H. *ggplot2: Elegant Graphics for Data Analysis.* New York: Springer-Verlag; 2016.
24. Snider KE, Becker S, Boyajian L, et al. Genotype and phenotype correlations in 417 children with congenital hyperinsulinism. *J Clin Endocrinol Metab.* 2013;98:E355-E363.
25. Flanagan SE, Patch AM, Locke JM, et al. Genome-wide homozygosity analysis reveals HADH mutations as a common cause of diazoxide-responsive hyperinsulinemic-hypoglycemia in consanguineous pedigrees. *J Clin Endocrinol Metab.* 2011;96:498-502.
26. Satapathy AK, Jain V, Ellard S, Flanagan SE. Hyperinsulinemic hypoglycemia of infancy due to novel HADH mutation in two siblings. *Indian Pediatr.* 2016;53:912-913.
27. van Hove EC, Hansen T, Dekker JM, et al. The HADHSC gene encoding short-chain L-3-hydroxyacyl-CoA dehydrogenase (SCHAD) and type 2 diabetes susceptibility: the DAMAGE study. *Diabetes.* 2006;55:3193-3196.
28. Barycki JJ, O'Brien LK, Bratt JM, et al. Biochemical characterization and crystal structure determination of human heart short chain L-3-hydroxyacyl-CoA dehydrogenase provide insights into catalytic mechanism. *Biochemistry.* 1999;38:5786-5798.
29. Gregersen N, Bross P, Jørgensen MM, Corydon TJ, Andresen BS. Defective folding and rapid degradation of mutant proteins is a common disease mechanism in genetic disorders. *J Inherit Metab Dis.* 2000;23:441-447.
30. Wu Y, Whitman I, Molmenti E, Moore K, Hippenmeyer P, Perlmutter DH. A lag in intracellular degradation of mutant α 1-antitrypsin correlates with the liver disease phenotype in homozygous PiZZ α 1-antitrypsin deficiency. *Proc Natl Acad Sci.* 1994;91:9014-9018.
31. O'Brien LK, Rinaldo P, Sims HF, et al. Fulminant hepatic failure associated with mutations in the medium and short chain L-3-hydroxyacyl-CoA dehydrogenase gene. *J Inherit Metab Dis.* 2000;23:127.
32. Bennett MJ, Russell LK, Tokunaga C, et al. Reye-like syndrome resulting from novel missense mutations in mitochondrial medium- and short-chain L-3-hydroxy-acyl-CoA dehydrogenase. *Mol Genet Metab.* 2006;89:74-79.
33. Fuchsberger C, Flannick J, Teslovich TM, et al. The genetic architecture of type 2 diabetes. *Nature.* 2016;536:41-47.
34. Narayan SB, Master SR, Sireci AN, et al. Short-chain 3-hydroxyacyl-coenzyme a dehydrogenase associates with a protein super-complex integrating multiple metabolic pathways. *PLoS One.* 2012;7:e35048.

SUPPORTING INFORMATION

Additional supporting information may be found online in the Supporting Information section at the end of this article.

How to cite this article: Velasco K, St-Louis JL, Hovland HN, et al. Functional evaluation of 16 SCHAD missense variants: Only amino acid substitutions causing congenital hyperinsulinism of infancy lead to loss-of-function phenotypes in vitro. *J Inherit Metab Dis.* 2021;44:240–252. <https://doi.org/10.1002/jimd.12309>